A nuclear lamin is required for cytoplasmic organization and egg polarity in *Drosophila*

Karen Guillemin*, Tyler Williams* and Mark A. Krasnow†*

Department of Biochemistry and Howard Hughes Medical Institute, Stanford University School of Medicine, Stanford, California 94305-5307, USA
**Current addresses: Department of Microbiology and Immunology, Stanford University School of Medicine, Stanford, California 94305-5124, USA (K.G.); Department of Molecular and Cell Biology, University of California, Berkeley, California 94720-3200, USA (T.W.)*
†e-mail: krasnow@cmgm.stanford.edu

Nuclear lamins are intermediate filaments that compose the nuclear lamina — the filamentous meshwork underlying the inner nuclear membrane — and are required for nuclear assembly, organization and maintenance. Here we present evidence that a nuclear lamin is also required for cytoplasmic organization in two highly polarized cell types. Zygotic loss-of-function mutations in the *Drosophila* gene encoding the principal lamin (Dm_0) disrupt the directed outgrowth of cytoplasmic extensions from terminal cells of the tracheal system. Germline mutant clones disrupt dorsal–ventral polarity of the oocyte. In mutant oocytes, transcripts of the dorsal determinant Gurken, a transforming growth factor-α homologue, fail to localize properly around the anterodorsal surface of the oocyte nucleus; their ventral spread results in dorsalized eggs that resemble those of the classical dorsalizing mutations *squid* and *fs(1)K10*. The requirement of a nuclear lamin for cytoplasmic as well as nuclear organization has important implications for both the cellular functions of lamins and the pathogenesis of human diseases caused by lamin mutations.

In a screen of tracheal P[*lacZ*] transposon insertions for mutations that alter the outgrowth of terminal branches of the *Drosophila* tracheal (respiratory) system, we identified mutations in a nuclear lamin gene. The original allele (*l(2)02459*) was a P[*lacZ*] insertion at cytologic position 25F1-2 that expresses LacZ in the tracheal cells that form terminal branches (Terminal-4 marker[1]); two additional alleles were obtained by imprecise excision of the transposon and four more were identified by complementation tests with existing lethal mutations in the 25F cytologic region. We named the gene *misguided (misg)*, because terminal branches in the mutants did not follow the normal projection patterns during branch outgrowth. In wild-type embryos, terminal branches grow out in stereotyped directions (Fig. 1a, c) towards specific targets on which they later ramify into extensive networks of fine terminal branches. They do not grow over or contact other branches, nor do they cross the dorsal or ventral midlines or enter target regions of other branches.

In *misg* mutant embryos, by contrast, terminal branches grew into the territory of, and contacted other terminal branches, occasionally crossing the midline or stalling during outgrowth (Fig. 1b, d). The original allele, *l(2)02459*, is weak and showed only occasional guidance defects. Six other alleles (*l(2)04643*, *ex91*, *ex98*, *sz18*, *sz9*, *a7*) showed a higher penetrance and expressivity of guidance defects (15–20% of branches affected at 25 °C; Table 1, and data not shown). The severity of the phenotype was not increased in *misg* hemizygotes ($misg^{4643}$/*Df(2L)cl-h3* and $misg^{4643}$/*Df(2L)GpdhA*), although it was increased substantially at elevated temperature (29 °C; and see below). No defects were seen in *misg* heterozygotes.

Terminal branches arise as long cytoplasmic extensions of tracheal terminal cells[2] (Fig. 1e). The cytoplasmic projections did not extend normally in *misg* mutants: 9% of terminal cells ($n = 144$) formed multiple cytoplasmic blebs, or thin spindly processes that grew in inappropriate directions (Fig. 1f) or stopped short before reaching their targets (Fig. 1g). Two per cent of terminal cells displayed defects in nuclear morphology, such as a spherical nucleus protruding off the main axis of the cell (Fig. 1g), but the disruption in cytoplasmic structure and outgrowth was more prevalent.

The sequence of the genomic DNA flanking the *misg* P[*lacZ*] alleles showed that both transposon insertions disrupted the transcription unit of lamin Dm_0 — a B-type lamin and the main constituent of the nuclear lamina[3] (Fig. 1h). All alleles examined showed reduced or no expression of lamin Dm_0 in germline clones (Fig. 2a, b, and Table 1). Furthermore, expression of a lamin Dm_0 transgene in the terminal cells of $misg^{4643}$ embryos using the Gal4/UAS system[4] ameliorated the mutant phenotype: at 29 °C, only 16% of dorsal branches ($n = 96$) were normal in control embryos carrying a terminal-cell-specific Gal4 driver, whereas 56% ($n = 192$) were normal in embryos carrying the Gal4 driver and UAS–lamin Dm_0. Thus, *misg* encodes lamin Dm_0 and it is required in tracheal cells for the structural organization and outgrowth of cytoplasmic processes. The residual defects in the rescue experiment may be due to suboptimal expression of the transgene or a cell non-autonomous component of the *misg* tracheal phenotype.

β-Galactosidase from the $misg^{2459}$ P[*lacZ*] is expressed strongly in tracheal terminal cells and weakly in epidermal cells[1], but there is a large maternal contribution of gene product and the protein is present at roughly equivalent levels in all embryonic cells including tracheal cells (ref. 3; and data not shown). To investigate the role of the maternally expressed gene product, we generated *misg* mutant germline clones using the dominant female sterile FLP/FRT system[5]. Females with germline clones of the two strongest alleles (*sz18*, *ex98*) did not deposit eggs. The mutant egg chambers showed severe defects in germline nuclear organization and morphology (Fig. 2c, d, and Table 1), consistent with known roles of lamin in nuclear assembly and maintenance, and the phenotypes of other lamin mutants[6–10].

Egg chambers of the other *misg* alleles (*a7*, *4643*, *2459*) showed much less severe or no germline nuclear abnormalities (Fig. 2e–h, and Table 1) and deposited eggs. Almost all the eggs showed striking defects in dorsal–ventral polarity (Fig. 3a–e, and Table 1). This ranged from mild dorsalization with expanded dorsal appendages (Fig. 3b), to strongly dorsalized, symmetrical eggs with a ring of dorsal appendage material surrounding the micropyle (Fig. 3d), resembling the phenotypes of the classic dorsalizing mutations *fs(1)K10* and *squid* (Fig. 3e; and ref. 11). Although dorsal–ventral patterning was

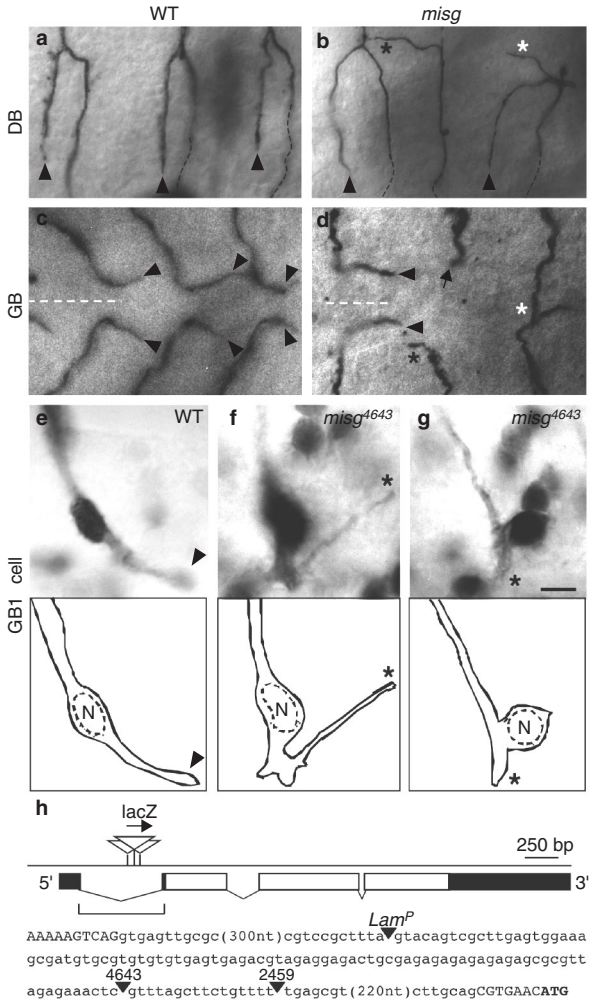

Figure 1 **Defects in directed outgrowth of tracheal terminal branches in *misg* mutants. a**, Lateral view (anterior left, dorsal up) of three dorsal branches (DB) in a stage 16 wild-type (WT) embryo stained with mAb2A12 to show tracheal lumen. Terminal branches (arrowheads) extend ventrally. Dashed lines indicate continuation of DBs out of focal plane. **b**, Similar view of a *misg*^{4643} embryo showing a misdirected (black asterisk) and an ectopic (white asterisk) terminal branch. **c**, Ventral view (anterior left) of three pairs of wild-type ganglionic branches (GB). GB terminal branches (arrowheads) extend posteriorly, parallel to the ventral midline (dashed line). **d**, Similar view of a *misg*^{ex91} embryo. Note the terminal branches extending anteriorly (black asterisk), crossing the midline and contacting the contralateral branch (white asterisk), and prematurely stalled (arrow). **e**, Micrograph (top) and tracing (bottom) of wild-type GB terminal cell carrying a *trachealess-lacZ* marker (1-eve-1; ref. 31) and stained for β-galactosidase to show tracheal cells and nuclei (N). A single cytoplasmic process (nascent terminal branch) extends posteriorly. The nucleus is ovoid and oriented in the axis of outgrowth. **f**, *misg*^{4643} GB cell showing thin, misdirected cytoplasmic process and multiple cytoplasmic blebs. **g**, *misg*^{4643} GB cell showing stalled outgrowth and round nucleus lying off the outgrowth axis. Scale bar, ~10 μm (**a**–**d**); ~5 μm (**e**–**g**). **h**, Positions of *misg*^{4643} and *misg*^{2459} P[*lacZ*] insertions in the lamin Dm_0 transcription unit. Genomic sequence of the bracketed region[32] is shown. Both insertions lie in the first intron, 258 and 232 bp upstream of the translation start site, as does a previously described weak mutation *Lam*^{P} (ref. 7). Open boxes, coding sequence; filled boxes, noncoding sequences. Lowercase, intron sequence; uppercase, exon sequence; boldface, start codon.

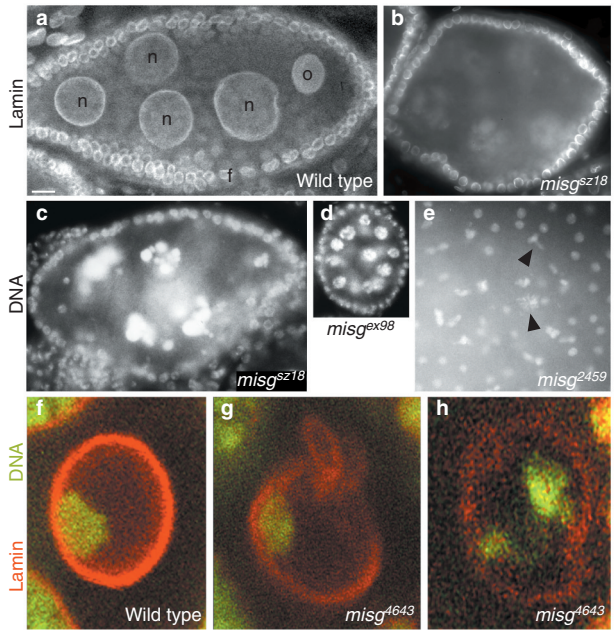

Figure 2 **Nuclear structure and division defects in *misg* germline clones. a**, Wild-type stage 6 egg chamber immunostained for lamin Dm_0. Lamin is detected at high levels throughout the oocyte nucleus (o) and at the periphery of the 15 nurse-cell nuclei (n; four are seen in this focal plane) and the nuclei of the somatic follicle cells (f) surrounding the germ line. **b**, *misg*^{sz18} germline clone. Lamin is greatly reduced or absent in the germline nuclei but is expressed normally in the follicle cells. The weak signal in the germline nuclei is probably spectral overlap from the DAPI channel (not shown). **c**, *misg*^{sz18} germline clone stained with DAPI to show DNA. Germline nuclei are disorganized. **d**, *misg*^{ex98} germline clone (stage 2). There are 16 large (nurse-cell) nuclei and no small (oocyte) nucleus, as in cytoplasmic dynein mutants[33]. **e**, DAPI stain of stage 2 embryo derived from *misg*^{2459} germline clone. Nuclear division is not synchronous and there are aberrant nuclear structures (arrowheads). **f**, Confocal micrograph of stage 4 wild-type oocyte nucleus stained for lamin Dm_0 (red) and DNA (propidium iodide, green). Nucleus is spherical and DNA is compacted to one side. **g**, **h**, Similar view of stage 4 *misg*^{4643} germline clones. Lamin staining is reduced in both, and there are abnormal nuclear protrusions resembling rabbit ears in **g** and aberrant DNA organization in **h**. The image in **h** is pixelated because the lamin signal was very weak and the gain on the lamin channel was increased maximally. Scale bar, ~10 μm (**a**); ~8 μm (**b**–**d**); ~4 μm (**e**); ~1.8 μm (**f**–**h**).

altered, anterior–posterior patterning seemed to be normal, as judged by normal micropyle and aeropyle morphology and normal localization of *oskar* messenger RNA in the oocyte (data not shown).

Dorsal–ventral polarity of the egg is controlled by the transforming growth factor-α homologue Gurken, which activates the epidermal growth factor receptor Torpedo on the overlying follicle cells, causing them to assume dorsal fates[11]. At stage 9 of oogenesis, the oocyte nucleus has migrated to a dorsal position in the anterior cortex of the cell, and *gurken* mRNA is tightly localized around the anterodorsal surface of the nucleus (Fig. 3f, h). We found that in *misg*^{4643} germline clones *gurken* RNA was sometimes less tightly associated with the oocyte nucleus (Fig. 3i) and spread more ventrally in the cell (Fig. 3g). The distribution of Gurken protein was also altered. In contrast to the tight dorsal stripe seen in wild-type egg chambers (Fig. 3j), Gurken staining in the mutant egg chambers was more diffuse, extending further ventrally but not as far posteriorly in the cell (Fig. 3k). This is similar to the defects in *gurken* transcript and protein localization seen in *fs(1)K10* and *squid* mutants, which lead to an increase in follicle cells adopting dorsal fates[12–15]. Thus, *misg* lamin is required for the proper cytoplasmic localization of a crucial determinant of egg polarity.

These results confirm the known functions of nuclear lamins in nuclear assembly and maintenance, but more importantly they

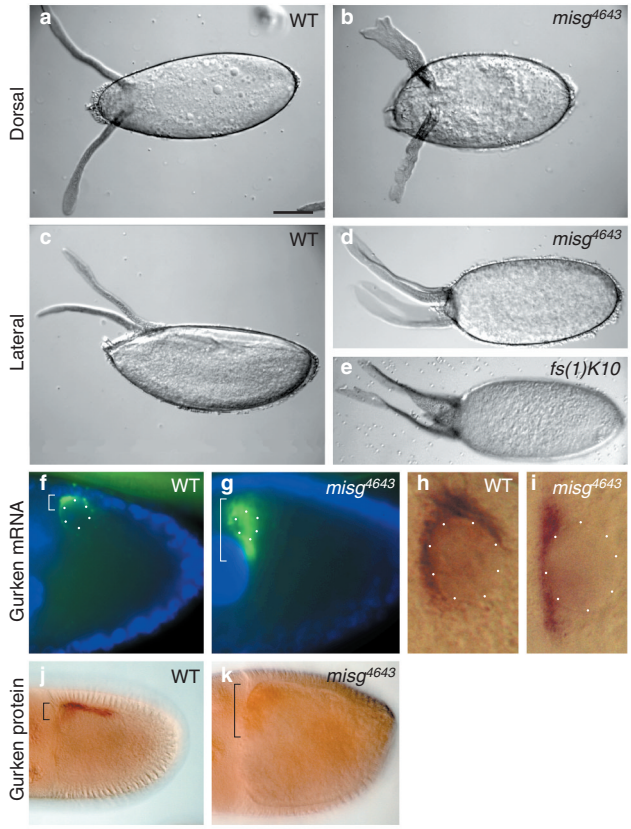

Figure 3 ***misg* germline clones give rise to dorsalized eggs. a**, Dorsal view (anterior left) of wild-type egg. A pair of dorsal appendages protrudes from the dorsal surface. **b**, Similar view of egg from *misg*^{4643} germline clone. Egg is partially dorsalized with thickened dorsal appendages. **c**, Lateral view (dorsal up) of wild-type egg. Ventral surface is rounded and dorsal surface is relatively flat. **d**, Same view of egg from *misg*^{4643} germline clone. Egg is almost fully dorsalized with ring of dorsal appendage encircling the anterior end and with symmetrical dorsal and ventral surfaces. **e**, Same view of egg from *fs(1)K10*^{LM00} mother for comparison. **f**, Lateral view (dorsal up) of stage 9 wild-type egg chamber hybridized with a probe for *gurken* RNA visualized by indirect immunofluorescence (green). Egg chamber was also stained with DAPI (blue) and lamin Dm_0 antiserum (not shown) to visualize the position of the oocyte nucleus (outlined with white dots). (Lamin Dm_0 staining is variable under these fixation conditions so was not used for the quantification of lamin Dm_0 levels in Table 1.) *gurken* RNA localizes to a tight cap (bracket) around the dorsal surface of the oocyte nucleus. **g**, *misg*^{4643} germline clone. *gurken* RNA extends ventrally in the cell. **h**, Close-up view of wild-type oocyte nucleus hybridized with *gurken* RNA probe and detected with alkaline phosphatase immunochemistry. Nucleus is outlined with white dots. **i**, *misg*^{4643} germline clone. Note *gurken* RNA is not tightly associated with the nucleus. **j**, Lateral view (dorsal up) of stage 10 wild-type egg chamber stained with anti-Gurken antiserum. Gurken protein localizes to a tight dorsal stripe (bracket) that extends posteriorly. **k**, *misg*^{4643} germline clone. Gurken protein is more diffuse, extending further ventrally (bracket) but not as far posteriorly as in wild type. Scale bar, ~100 μm (**a**–**e**); ~30 μm (**f**, **g**); ~15 μm (**h**, **i**); ~40 μm (**j**, **k**).

show that a nuclear lamin can also influence cytoplasmic organization in at least two different *Drosophila* cell types, the oocyte and tracheal terminal cells. How might *misg* lamin, the main constituent of the nuclear lamina, affect cytoplasmic organization? One possibility is that a small, as yet undetected cellular fraction of this lamin localizes and functions in the cytoplasm. Another possibility is that the nuclear protein is required for correct expression of one or more cytoplasmic factors(s). Lamins can bind chromatin directly or through interactions with chromatin-binding nuclear membrane proteins, so they can influence chromosome organization and possibly gene expression[6,10,16]. *gurken* transcripts are synthesized in the oocyte nucleus and must interact with the Squid hnRNP protein and possibly K10, a putative RNA-binding protein, in order to localize properly after export into the cytoplasm[17,18]. Oocyte nuclei with reduced *misg* lamin may synthesize *gurken* transcripts normally but fail to process them correctly, resulting in cytoplasmic mislocalization. The effect of *misg* mutations on gene expression would have to be selective, because the affected eggs and tracheal cells retain many normal aspects of cell differentiation and function.

The cytoplasmic defects in *misg* mutants might also be explained if lamin-dependent connections exist between the nucleus and cytoplasm that are necessary for cellular organization. The nucleus is physically connected to the rest of the cell through actin filaments, intermediate filaments, microtubules and the endoplasmic reticulum[19]. Indeed, it has been proposed that an intermediate filament network extends from the plasma membrane into the nucleus, possibly passing through nuclear pores to interact with the underlying lamina[20]. In lamin-depleted oocytes and tracheal cells, such connections may be compromised, with consequent loss of cytoplasmic organization.

Whatever the molecular explanation, the finding that different cellular phenotypes predominate in *misg* alleles of different strengths suggests that *misg* lamin may have several functions, each requiring a different threshold level of the protein. Because cytoplasmic defects in *misg* alleles can occur without grossly altering nuclear structure, they seem to be the most sensitive to lamin depletion.

The requirement of a nuclear lamin for cytoplasmic organization and cell polarity might help explain the pathogenesis of several human diseases recently found to be caused by mutations in the lamin A/C gene. These include an autosomal dominant adult-onset cardiomyopathy[21], a rare familial lipodystrophy[10] and the autosomal dominant form of Emery–Dreifuss muscular dystrophy (EDMD)[22], as well as a mouse model of EDMD generated by targeted disruption of the homologous gene[9]. It has been difficult to explain how defects in a nuclear lamin give rise to these diseases because nuclear structure or organization is not obviously altered in affected individuals[23]. Perhaps, as with the less severe *misg* mutations, cytoplasmic defects predominate. For example, muscle cells are highly organized and exhibit coordinated transcript localization and translation at sites where proteins are required in the cell[24], such as the sarcolemma in which dystrophin, β-dystroglycan and other genes implicated in muscular dystrophy localize[25,26]. Localization of these or other cytoplasmic components may be perturbed in EDMD patients, like *gurken* transcripts in *misg* mutant oocytes. □

Methods

Fly strains and genetics.

misg^{2459} and *misg*^{4643} correspond to *l(2)02459* and *l(2)04643* (ref. 27). Several P-transposase-induced excisions of the *misg*^{2459} P[*lacZ*] element reverted the lethality; imprecise excisions created additional lethal alleles, two of which (*misg*^{ex91} and *misg*^{ex98}) exhibited strong *misg* phenotypes. *misg*^{ex18}, *misg*^{ex7}, *misg*^{ex9} are ethylmethane-sulphonate-induced alleles from the 25F region[28] that failed to complement the lethality of *misg*^{4643}. All three exhibited the same tracheal phenotype, but *misg*^{ex9} contained a second closely linked lethal mutation and was not analysed further. We recombined *misg* alleles onto the FRT40A chromosome and created germline clones by the dominant female sterile FLP/FRT technique[5].

Immunostaining, *in situ* hybridization and histology.

Whole-mount embryos were fixed and stained as described[1] using antibodies against a tracheal luminal antigen (mAb2A12, 1:5 dilution), β-galactosidase (from Cappell, 1:1500) and lamin Dm_0 (mAb ADL84 from P. Fisher, 1:100). Ovaries were dissected in PBS, fixed in 4% formaldehyde, stained with mAb ADL84 and Cy3- or Cy5-conjugated secondary antibody, and counterstained with 4′,6-diamidino-2-phenylindole (DAPI) or propidium iodide as described[29]. We fixed and stained ovaries with a rabbit polyclonal anti-Gurken antiserum (1:1000) and horseradish peroxidase (HRP) immunohistochemistry as described[14]. *In situ* hybridization of ovaries was performed using digoxigenin-labelled *gurken* and *oskar* RNA probes and alkaline phosphatase immunohistochemistry[30] or indirect immunofluorescence using anti-digoxigenin antibody coupled to HRP (Boerhinger Mannheim) and tyramide/FITC immunochemistry (NEN Life Science). To analyse egg morphology, we mounted the eggs in Hoyer's medium.

Table 1 Zygotic and maternal *misg* phenotypes

	Allele	Mutagen	Zygotic	Maternal*			
			Tracheal guidance defects†	Lamin egg chamber expression‡	Egg chamber morphology	Egg production	Egg polarity‡‡
Increasing severity ↓	Wild type (Canton S)	None	<1%	Normal	Normal§	Normal	Normal (0% eggs affected)
	misg^{2459} (*1(2)02459*)	P[*lacZ*]	2%	n.d.	Normal	Reduced	Weakly dorsalized (82%)
	misg^{4643} (*1(2)04643*)	P[*lacZ*]	20%	Reduced	Occasional oocyte differentiation and nuclear morphology defects¶	Greatly reduced	Dorsalized (86%)
	misg^{a7}	EMS	17%	Reduced	Frequent oocyte differentiation defects#	Greatly reduced	Strongly dorsalized (100%)
	misg^{ex98}	P[*lacZ*] excision	15%	Reduced	Early development arrest**	None	(no eggs)
	misg^{sz18}	EMS	19%	Undetectable	Severe nuclear disorganization††	None	(no eggs)

* Egg chamber and egg phenotypes of homozygous *misg* germ line clones.
† Percentage of misguided and stalled dorsal ganglionic branches in homozygous embryos at 25 °C ($n \geq 170$ branches).
‡ Lamin Dm_0 levels were analysed in egg chambers fixed and immunostained as in Fig. 2a, b. Egg chambers from wild-type and *misg* alleles were processed in parallel, and the results were consistent for each allele.
§ Wild-type egg chambers have 1 small (diploid) oocyte nucleus and 15 large (polyploid) nurse cell nuclei.
¶ Occasional egg chambers with 2 small and 14 large nuclei. See Fig. 2g, h for examples of nuclear morphology defects.
# Frequent egg chambers with 2 small and 14 large nuclei, or 3 small and 13 large nuclei.
**Arrested at stage 2 with 16 similarly sized nuclei per egg chamber (Fig. 2d).
†† See Fig. 2c.
‡‡ Mutant eggs displayed a range of dorsal–ventral polarity defects; the percentage of mutant eggs affected is shown. Affected eggs fell into four classes: expanded dorsal appendages (Class I; see Fig. 3b); single fused or circumferential dorsal appendage (II, see Fig. 3d); multiple dorsal appendages (III); no dorsal appendage (IV). The number of mutant eggs scored (*n*) and percentage in each class were: *misg*^{2459} (n = 157): I (64%), II (12%), III (5%), IV (1%). *misg*^{4643} (n = 97): I (55%), II (18%), III (9%), IV (4%). *misg*^{a7} (n = 34): I (44%), II (41%), III (9%), IV (6%).
n.d., not determined.

Molecular characterization and rescue of *misg* mutations.

Plasmid rescue was performed on genomic DNA from *misg*^{2459} and *misg*^{4643}, and the DNA sequence flanking the P[*lacZ*] ends was determined by standard methods. Four genomic and twelve complementary DNA clones (including J14-5A, J14-3A) were obtained by screening genomic (J. Tamkun) and embryonic cDNA (K. Zinn) libraries with fragments of flanking DNA. We created a UAS–lamin Dm_0 expression construct (pKG4019) by inserting an *Eco*RI fragment from cDNA J14-3A into the pUAST vector[4]. P-element-mediated transformation was used to generate UAS–lamin-6, an insertion on chromosome 3. A terminal-cell-specific GAL4 driver strain was generated by inserting the *Drosophila* hsp70 minimal promoter (–50 to +90) upstream of the Gal4 coding sequence in pGaTB (ref. 4) to create pKG4021. The hsp70 promoter–Gal4 sequence was then subcloned into a Casper4 vector to create pKG4022, and a 4.4-kilobase *Eco*RI fragment upstream of the *blistered* (*pruned*) coding sequence[2], which contains a terminal-cell-specific enhancer, was introduced into the unique *Eco*RI site of pKG4022. We used P-element-mediated transformation of the resultant plasmid (pKG4023) to generate Term Gal4-26, an insertion on chromosome 3 that expresses strongly in tracheal terminal cells beginning at stage 13, and weakly in somatic muscles beginning at stage 15. Rescue of the tracheal *misg* phenotype was analysed in embryos from the cross: *misg*^{4643}*/CyO P[actin::lacZ]; TermGal4-26* X *misg*^{4643}*/CyO P[actin::lacZ]; UAS–lamin-6*. The cross was done at 29 °C, which exacerbates the *misg* phenotype and increases Gal4 activity.

RECEIVED 2 APRIL 2001, REVISED 4 MAY 2001, ACCEPTED 29 MAY 2001,
PUBLISHED 16 AUGUST 2001.

1. Samakovlis, C. *et al. Development* **122,** 1395–1407 (1996).
2. Guillemin, K. *et al. Development* **122,** 1353–1362 (1996).
3. Gruenbaum, Y. *et al. J Cell Biol* **106,** 585–596 (1988).
4. Brand, A. H. & Perrimon, N. *Development* **118,** 401–415 (1993).
5. Chou, T. B. & Perrimon, N. *Genetics* **144,** 1673–1679 (1996).
6. Cohen, M., Lee, K. K., Wilson, K. L. & Gruenbaum, Y. *Trends Biochem. Sci.* **26,** 41–47 (2001).
7. Lenz, B. B. *et al. J. Cell Biol.* **137,** 1001–1016 (1997).
8. Liu, J. *et al. Mol. Biol. Cell* **11,** 3937–3947 (2000).
9. Sullivan, T. *et al. J. Cell Biol.* **147,** 913–920 (1999).
10. Wilson, K. L., Zastrow, M. S. & Lee, K. K. *Cell* **104,** 647–650 (2001).
11. Nilson, L. A. & Schupbach, T. *Curr. Top. Dev. Biol.* **44,** 203–243 (1999).
12. Roth, S., Neuman, S. F., Barcelo, G. & Schupbach, T. *Cell* **81,** 967–978 (1995).
13. Roth, S. & Schupbach, T. *Development* **120,** 2245–2257 (1994).
14. Peri, F., Bokel, C. & Roth, S. *Mech. Dev.* **81,** 75–88 (1999).
15. Serano, T. L., Karlin-McGinness, M. & Cohen, R. S. *Mech. Dev.* **51,** 183–192 (1995).
16. Marshall, W. F. & Sedat, J. W. *Results Probl. Cell Differ.* **25,** 283–301 (1999).
17. Saunders, C. & Cohen, R. S. *Mol. Cell* **3,** 43–54 (1999).
18. Norvell, A., Kelley, R. L., Wehr, K. & Schupbach, T. *Genes Dev.* **13,** 864–876 (1999).
19. Maniotis, A. J., Chen, C. S. & Ingber, D. E. *Proc. Natl Acad. Sci. USA* **94,** 849–854 (1997).
20. Fey, E. G., Wan, K. M. & Penman, S. *J. Cell Biol.* **98,** 1973–1984 (1984).
21. Fatkin, D. *et al. N. Engl. J. Med.* **341,** 1715–1724 (1999).
22. Bonne, G. *et al. Ann. Neurol.* **48,** 170–180 (2000).
23. Wilson, K. L. *Trends Cell Biol.* **10,** 125–129 (2000).
24. Fulton, A. B. *J. Cell Biochem.* **52,** 148–152 (1993).
25. Mitsui, T. *et al. J. Neuropathol. Exp. Neurol.* **56,** 94–101 (1997).
26. Toniolo, D. & Minetti, C. *Curr. Opin. Genet. Dev.* **9,** 275–282 (1999).
27. Spradling, A. C. *et al. Proc. Natl Acad. Sci. USA* **92,** 10824–10830 (1995).
28. Szidonya, J. & Reuter, G. *Genet. Res.* **51,** 197–208 (1988).
29. Verheyen, E. & Cooley, L. in *Drosophila melanogaster: Practical Uses in Cell and Molecular Biology* (eds Goldstein, L. S. B. & Fyrberg, E. A.) 545–561 (Academic, New York, 1994).
30. Kopczynski, C. C., Davis, G. W. & Goodman, C. S. *Science* **271,** 1867–1870 (1996).
31. Perrimon, N., Noll, E., McCall, K. & Brand, A. *Dev. Genet.* **12,** 238–252 (1991).
32. Osman, M., Paz, M., Landesman, Y., Fainsod, A. & Gruenbaum, Y. *Genomics* **8,** 217–224 (1990).
33. McGrail, M. & Hays, T. S. *Development* **124,** 2409–2419 (1997).

ACKNOWLEDGEMENTS
We thank P. Fisher, T. Schubach and N. Perrimon for antibodies and fly strains; and I. Davis, Y. Gruenbaum, J. Sedat, K. Wilson, and members of the Krasnow lab for helpful discussions. This work was supported by a grant from the NIH. M.A.K. is an investigator of the Howard Hughes Medical Institute.
Correspondence and requests for materials should be addressed to M.A.K.